Journal of Molecular Imaging & Dynamics

Iizuka et al., J Mol Imaging Dynamic 2017, 7:2
DOI: 10.4172/2155-9937.1000137

Research Article Open Access

Visual and Quantitative Assessment of a New Anisotropic Diffusion Filter (Statistical Transfer with Optimizing Noise and Edge Sensing) for Positron Emission Tomography

Hitoshi Iizuka[1], Tomohiro Kaneta[1*], Matsuyoshi Ogawa[1], Nobutoku Motomura[2], Tetsu Arisawa[1], Ayako Hino-Shishikura[1], Keisuke Yoshida[1] and Tomio Inoue[1]

[1]Department of Radiology, Yokohama City University, Yokohama, Japan

[2]Department of Nuclear Medicine System and Development, Toshiba Medical Systems Corporation, Tochigi, Japan

***Corresponding author:** Tomohiro Kaneta, Department of Radiology, Yokohama City University, 3-9 Fukuura, Kanazawa-Ku, Yokohama, 236-0004, Japan, Tel: 81-45-787-2696, E-mail: kaneta@yokohama-cu.ac.jp

Rec date: Oct 26, 2017; **Acc date:** Nov 04, 2017; **Pub date:** Nov 08, 2017

Abstract

Post-filtering with a Gaussian filter is commonly used to reduce noise in positron emission tomography (PET) images. However, its non-selective smoothing obscures the edges of lesions or organs. We compared the performance of a newly developed anisotropic diffusion filter called "Statistical Transfer with Optimizing Noise and Edge Sensing" (STONES) with that of the Gaussian filter for small lesions on PET images. We selected seven PET/computed tomography (CT) image slices of the lungs from three patients with multiple lung metastases. For each slice, the lesion detection rates by two physicians (A and B) were compared for Gaussian- and STONES-filtered PET images. The maximum standardized uptake (SUV_{max}) values of the detected lesions were also compared for non-, Gaussian-, and STONES-filtered images. Physician A detected 19 lesions in the Gaussian-filtered images and 23 lesions in the STONES-filtered images, while Physician B detected 14 lesions in the Gaussian-filtered images and 19 lesions in the STONES-filtered images. SUV_{max} for the STONES-filtered images was significantly higher and closer to that of the non-filtered images compared to those for the Gaussian-filtered images. STONES improved the detection rate and increased SUV_{max} in comparison with Gaussian filter. Thus, it should be more advantageous for the detection of small lesions with PET.

Keywords: STONES; Anisotropic diffusion filter; Gaussian filter; FDG-PET; Edge preservation; Lung

Introduction

Positron emission tomography (PET) is a medical imaging modality with proven clinical value for the detection, staging, and monitoring of a wide variety of diseases [1,2]. The detection of an abnormal uptake is a critical process in interpreting PET images. However, such images intrinsically contain statistical noise, which sometimes makes it difficult to decide whether or not there is an abnormal uptake. PET images are produced by reconstructing raw sinogram data acquired from a scanner [3]. Filtered back projection (FBP) used to be the algorithm of choice for PET image reconstruction. However, iterative reconstruction algorithms such as ordered-subset expectation maximization (OSEM) [4] have replaced FBP because they handle Poisson noise in the sinogram data more optimally, which improves the image signal-to-noise ratio (SNR) and eliminates streaky artifacts [5]. On the other hand, a higher injected activity is known to correlate with lower levels of noise. However, it is not realistic to simply increase activity owing to radiation exposure and the cost of 18F-fluorodeoxyglucose (FDG) production [6]. The acquisition time is another factor that affects the level of noise in a PET image. In the practical range, a longer acquisition time correlates with lower levels of noise [7]. However, increasing the acquisition time tends to cause patient discomfort and motion artifacts [8]. Another approach to improving the SNR in PET is to apply a smoothing filter after reconstruction [9-11]. The Gaussian filter is widely used as a post-filtering method for noise reduction. However, it obscures the edges of areas with an abnormal uptake because the smoothing strength is directly proportional to the local image gradient, which means that isotropic diffusion filters smoothen edges as well as noise in lesions or the background. In contrast, anisotropic diffusion filters [12,13] can preserve edges while they smoothen areas with noise. This is because the diffusion process for this type of filter is tuned to return large values in regions with no or small intensity fluctuations and small values in areas with large intensity variations [13]. Toshiba Medical Systems (Tochigi, Japan) recently developed an anisotropic diffusion filter for PET that is based on the adaptive iterative dose reduction (AIDR) algorithm [14] for use in its computed tomography (CT) scanners. The new filter is called "Statistical Transfer with Optimizing Noise and Edge Sensing" (STONES). Theoretically, this new filter can improve the lesion detection performance, particularly for small lesions. In this study, we evaluated its effects on PET images of patients with multiple metastatic lung tumors by visual assessment and quantitative indices. We compared the results with those of a Gaussian filter, which is the standard post-filter used at our institution.

Materials and Methods

Subjects

Our institution is a university hospital with a large number of cancer patients. There are two PET/CT scanners (Aquiduo and Celesteion, both manufactured by Toshiba Medial Systems), and PET/CT scans were obtained from either of them randomly. STONES is currently available only on Celesteion. Among the patients who underwent FDG-PET/CT scans on Celesteion at our institution

between September 2015 and May 2016, nine had multiple lung tumors. Patients without appropriate image slices were excluded before analysis of the PET images. The institutional review board approved this study (#B160301013), and written informed consent was waived because of the retrospective design.

Methods

Image acquisition, reconstruction, and filtering: Patients were intravenously injected with 3.7 MBq/kg of 18F-FDG after fasting for at least 4 h. Scans were performed on Celesteion approximately 1 h after FDG administration. PET data were acquired with the following parameter values: data acquisition at 120 seconds per bed position, field of view of 400–700 mm, three iterations, 10 subsets, matrix size of 175 × 175, and reconstruction by attenuation-weighted ordered-subsets expectation maximization. CT data were acquired at 120 kVp with an automatic exposure control system and a beam pitch of 0.938 in a 16-detector row mode with a 2-mm slice thickness. We obtained two series of post-filtered PET images for each scan processed with a 6-mm full-width at half-maximum (FWHM) Gaussian filter and STONES. Example images are shown in Figures 1 and 2.

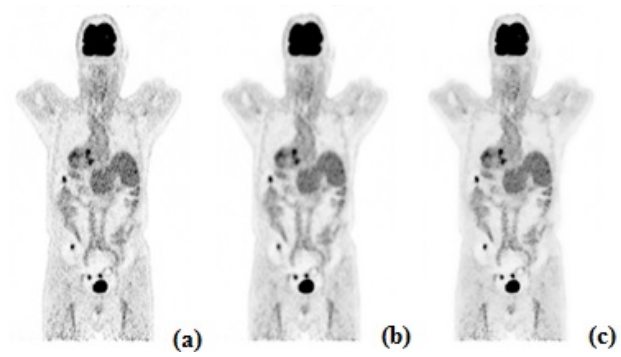

Figure 1: Examples of coronal FDG-PET images: (a) Non-post-filtered coronal image and its post-filtered images processed with (b) a Gaussian filter and (c) STONES. Noise is reduced in both post-filtered images, while the edges are better preserved in the STONES-filtered image.

Figure 2: Examples of axial FDG-PET images processed with the Gaussian filter and STONES and the corresponding CT image of the same slice. (c) shows a nodule in the left lung, (b) shows a small area with increased uptake corresponding to the nodule, and (a) shows that the area is blurred.

Slice selection and image analysis: We selected seven slices (slices 1-7) from three patients with 1-20 nodular lesions, all of which were 15 mm or less in diameter on CT. Thus, we obtained 14 PET images in total with two types of post-filtered images for each selected slice. Slices from the remaining six patients were not selected because they did not meet the conditions regarding lesion numbers and size or included lesions in contact with another, which could cause a difference in lesion counts. The PET images were assessed by two board-certified nuclear medicine physicians (Physicians A and B) who were blind to the filter type and corresponding CT image. Fourteen PET images were randomly shown to each physician, and they were asked to detect an abnormal uptake. The locations of all abnormal uptakes were recorded. The results were compared with the corresponding CT. When a lesion existed on CT at the location with an abnormal uptake, the PET finding was classified as a true positive. On the other hand, when a lesion did not exist on CT, the PET finding was classified as a false positive. When readers did not detect lesions on CT in the PET image, the PET finding was classified as a false negative. The lesion detection rate was defined as the number of true positives divided by the number of corresponding nodular lesions on CT.

Statistical analysis

The Wilcoxon signed-rank test was used to compare the lesion detection rates and numbers of false positive uptakes for the different filter types. The Wilcoxon signed-rank test and Mann–Whitney U test were used to compare the maximum standardized uptake (SUV_{max}) values of the detected lesions on the original non-post-filtered images and two types of post-filtered images. The correlation of SUV_{max} among the three types of PET images was also evaluated.

Results

Visual assessment

Physician A detected 19 lesions on PET images processed with the Gaussian filter and 23 lesions on PET images processed with STONES. Physician B detected 14 lesions on PET images processed with the Gaussian filter and 19 lesions on PET images processed with STONES (kappa values of 0.65 and 0.76 for images processed with STONES and the Gaussian filter, respectively). Table 1 presents the number of detected areas with an abnormally increased uptake on PET, the number of nodular lesions on CT, the lesion detection rate, and the number of false-positive lesions for each image. There was a significant difference between the lesion detection rates for PET images processed with the two filters (0.0416). There was no significant difference between the numbers of areas with a false-positive uptake (0.0937).

Quantitative assessment

Table 2 presents SUV_{max} for the detected lesions on PET images with no post-filtering, those processed with the Gaussian filter, and those processed with STONES (SUV_{max} (N), SUV_{max} (G), and SUV_{max} (S), respectively). SUV_{max} (S) was significantly higher than SUV_{max} (G) (P=0.001). SUV_{max} (S) was higher for 17 out of 23 lesions, while SUV_{max} (G) was higher for only six lesions. The average SUV_{max} was significantly higher for the former lesions than the latter lesions, as shown in Figure 3 (P=0.0423). A positive correlation was found between the values SUV_{max} (S) – SUV_{max} (G) and SUV_{max} (N), as shown in Figure 4 (R2=0.62, P<0.001). None of the detected lesions showed an increase in SUV_{max} with post-filtering regardless of the filter type.

	Number of Nodular Lesions (CT)	Physician A						Physician B					
		Gaussian			STONES			Gaussian			STONES		
		Number of True-Positives	Lesion Detection Rate (%)	Number of False-Positives	Number of True-Positives	Lesion Detection Rate (%)	Number of False-Positives	Number of True-Positives	Lesion Detection Rate (%)	Number of False-Positives	Number of True-Positives	Lesion Detection Rate (%)	Number of False-Positives
Slice 1	1	0	0	0	1	100	0	0	0	0	1	100	0
Slice 2	1	1	100	0	1	100	4	1	100	3	1	100	3
Slice 3	1	1	100	0	1	100	2	1	100	1	1	100	1
Slice 4	15	3	20	0	5	33	0	2	13	0	4	27	0
Slice 5	3	2	67	1	2	67	0	2	67	1	2	67	0
Slice 6	14	7	50	2	8	57	4	5	36	0	7	50	1
Slice 7	10	5	50	1	5	50	1	3	30	0	3	30	0
Total	45	19	42	4	23	51	11	14	31	5	19	42	5

Table 1: The results of image interpretation by two physicians showing the number of nodular lesions on CT, the number of detected areas with abnormally increased uptakes on PET, lesion detection rate and the number of the false-positive for each image.

	SUV_{max} (N)	SUV_{max} (G)	SUV_{max} (S)
Lesion 1	0.85	0.37	0.58
Lesion 2	1.67	0.61	1.17
Lesion 3	1.12	0.63	0.65
Lesion 4	1.14	0.84	0.95
Lesion 5	1.54	1.13	1.24
Lesion 6	1.37	1.18	1.13
Lesion 7	1.04	0.75	0.75
Lesion 8	1.37	0.92	0.94
Lesion 9	2.19	1.47	1.65
Lesion 10	1.39	0.93	0.91
Lesion 11	1.15	1.04	1.06
Lesion 12	3.27	1.84	2.18
Lesion 13	5.96	4.74	5.85
Lesion 14	2.24	1.73	2.14
Lesion 15	1.25	0.81	0.84
Lesion 16	1.88	1.29	1.26
Lesion 17	1.09	0.93	0.87

Lesion 18	1.05	0.65	0.60
Lesion 19	2.87	1.96	2.38
Lesion 20	5.04	3.91	4.61
Lesion 21	4.42	3.09	3.66
Lesion 22	2.27	1.56	1.71
Lesion 23	5.96	5.01	5.30

Table 2: SUV_{max} (N), SUV_{max} (G) and SUV_{max} (S) of each lesion.

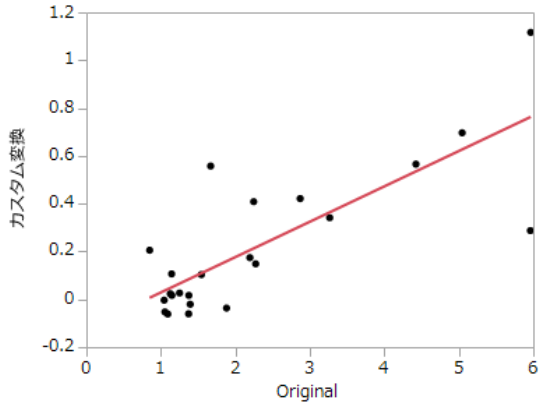

Figure 3: Positive correlation between the values SUV_{max} (S) – SUV_{max} (G) and SUV_{max} (N).

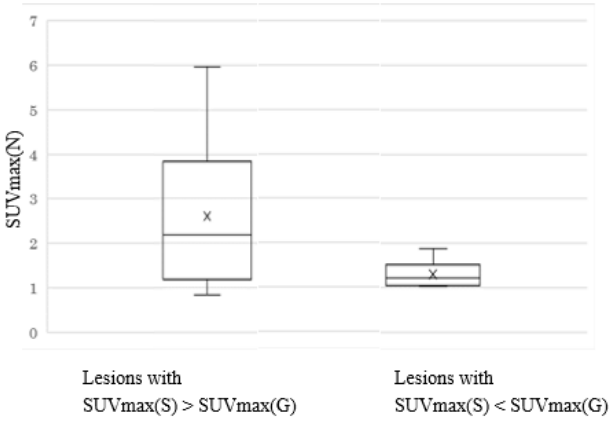

Figure 4: Distribution of SUV_{max} (N) to compare two groups of lesions: one with SUV_{max} (S) larger than SUV_{max} (G), and the other with SUV_{max} (S) smaller than SUV_{max} (G).

Discussion

In this study, we first investigated the visual effect of STONES on PET images in comparison with the Gaussian filter. The Gaussian filter smoothens the count of lesion edges, which can degrade the lesion detection performance. STONES was designed to address this phenomenon by edge preservation. The results in Table 1 indicate that STONES may improve the lesion visibility in PET images. The better visual assessment results were assumed to be due to the edge preservation by STONES. Because the detection rates of both physicians improved compared with the Gaussian filter for the same slices, the improved visibility appears to be due to specific conditions. Because there was concern that SUV may be decreased by the smoothing effect of the filters, we then assessed the change in SUV_{max} of the detected lesions by post-filtering, which should demonstrate the effect of edge preservation by STONES against this phenomenon. Because SUV in FDG-PET was used as a quantitative index to show the metabolic activity, the change due to filtering should be minimized. The results in Table 2 indicate that the change in SUV_{max} with STONES was less than that with the Gaussian filter. No lesion showed an increase in SUV_{max} with post-filtering. These characteristics were more obvious for lesions with a large SUV_{max} (N), as shown in Figure 3. For some lesions with SUV_{max} (N)<2, SUV_{max} (S) was less than SUV_{max} (G), as shown in Figures 3 and 4. No image slice saw a lower lesion detection rate with STONES than with the Gaussian filter. This may imply that not only a higher SUV_{max} but also better edge preservation and/or background smoothing can improve the lesion detection rate.

We chose the lung as the target organ of this study because of the homogeneity of its background uptake on FDG-PET and the simplicity of judging whether or not there actually is a lesion by referring to corresponding CT images obtained prior to PET data acquisition. This is difficult for lesions of other organs such as the liver and pancreas.

The limitations of this study include the small number of subjects and single-slice image interpretation. More lesions and patients are required for a more precise statistical analysis and assessment of the effects of body sizes, respectively. In clinical practice, PET images are usually interpreted in series, not as independent single images. The single-slice interpretation in this study may have reduced the detection rate and increased the false positives. Additionally, the results of the quantitative assessment cannot be easily interpreted because SUV_{max} is not the only index available for uptake quantification. SUV_{mean} (mean of SUV for each voxel within a lesion), SUV_{peak} (Average SUV within a 1 cm^3 sphere centered in the highest uptake region of the lesion [15]), and SUV_{total} (sum of SUV for each voxel within a lesion) can also be used for similar purposes. In this study, we chose SUV_{max} as the first step to investigate the effects of STONES on SUV because it is by far the most widely used index in analyzing tumors in quantitative 18F-FDG oncology studies [15]. However, SUV_{max} is vulnerable to statistical noise, which can be attributed to its single-pixel (voxel)

nature [16]. Computer simulations have shown that SUV_{max} increases with the image noise [17]. Also, it has been reported that different SUV measures result in a considerable degree of variation [18]. Thus, we need further investigation in order to decide what the results in the present study mean.

Conclusion

In summary, STONES may be a more suitable post-filter for FDG-PET than the Gaussian filter when evaluating lung nodules and may improve the lesion detection performance. A larger-scale study is required in order to use it in clinical practice.

Acknowledgments

Funding

Tomohiro Kaneta has received a research fund from Toshiba Medical Systems Corporation.

Competing interests

This work was performed as a part of a collaborative research project with Toshiba Medical Systems Corporation. Nobutoku Motomura is an employee of Toshiba Medical Systems Corporation.

References

1. Tong S, Alessio AM, Kinahan PE (2011) Image reconstruction for PET/CT scanners: Past acheivements and future challenges. Imaging Med. 2: 529-545.
2. Spieth ME, Kasner DL (2002) A tabulated summary of the FDG PET Literature. J Nucl Med. 43: 439-441.
3. Alrefaya M, Sahli H, Vanhamel I, Hao DN (2009) A nonlinear probabilistic curvature motion filter for positron emission tomography images. Lect Notes Comput Sci SSVM: 212-223.
4. Hudson HM, Larkin RS (1994) Accelerated image reconstruction using ordered subsets of projection data. IEEE Trans Med Imaging 13: 601-609.
5. Søndergaard HM, Madsen MM, Boisen K, Bøttcher M, Schmitz O, et al. (2007) Evaluation of iterative reconstruction (OSEM) versus filtered back-projection for the assessment of myocardial glucose uptake and myocardial perfusion using dynamic PET. Eur J Nucl Med Mol Imaging 34: 320-329.
6. Everaert H, Vanhove C, Lahoutte T, Muylle K, Caveliers V, et al. (2003) Optimal dose of 18F-FDG required for whole-body PET using an LSO PET camera. Eur J Nucl Med Mol Imaging. 30: 1615-1619.
7. Brown C, Dempsey M, Gillen G, Elliott AT (2001) Investigation of 18 F-FDG 3D mode PET image quality versus acquisition time. Nuclear Medicine Communications 31: 3-8.
8. McDermott GM, Chowdhury FU, Scarsbrook AF (2013) Evaluation of noise equivalent count parameters as indicators of adult whole-body FDG-PET image quality. Ann Nucl Med. 27: 855-861.
9. Chan C, Fulton R, Barnett R, Feng DD, Meikle S (2014) Post reconstruction nonlocal means filtering of whole-body PET with an Anatomical Prior. IEEE Trans Med Imaging 33: 636-650.
10. Nuyts J, Fessler JA (2003) A penalized-likelihood image reconstruction method for emission tomography, compared to post smoothed [maxim]um-likelihood with matched spatial resolution. IEEE Trans Med Imaging 22: 1042-1052.
11. Nuyts J, Baete K, Beque D, Dupont P (2005) Comparison between MAP and post processed ML for image reconstruction in emission tomography when anatomical knowledge is available. IEEE Trans Med Imaging 24: 667-675.
12. Perona P, Malik J (1990) Scale-space and edge detection using anisotropic diffusion. IEEE Trans Pattern Anal Mach Intell. 12: 629-639.
13. Chan C, Fulton R, Feng DD, Meikle S (2009) Regularized Image Reconstruction with an Anatomically Adaptive Prior for Positron Emission Tomography. Phys Med Biol. 54: 7379-7400.
14. Yang Z, Silver MD, Noshi Y (2011) Adaptive weighted anisotropic diffusion for computed tomography denoising. 11th Int Meet Fully Three-Dimensional Image Reconstr Radiol Nucl Med Potsdam Ger 11-15.
15. Wahl RL, Jacene H, Kasamon Y, Lodge MA (2009) From RECIST to PERCIST: Evolving considerations for PET response criteria in Solid Tumors. J Nucl Med. 50: 122S-150S.
16. Lodge MA, Chaudhry MA, Wahl RL (2012) Noise considerations for PET quantification using [maximum and] peak standardized uptake value. J Nucl Med. 53: 1041-1047.
17. Boellaard R, Krak NC, Hoekstra OS, Lammertsma AA (2004) Effects of noise, image resolution, and ROI definition on the accuracy of standard uptake values: A simulation study. J Nucl Med. 45: 1519-1527.
18. Vanderhoek M, Perlman SB, Jeraj R (2012) Impact of the definition of peak standardized uptake value on quantification of treatment response. J Nucl Med. 53: 4-11.